DNA mismatch repair controls the mutagenicity of Polymerase ζ-dependent translesion synthesis at methylated guanines

Tsaalbi-Shtylik, A.; Mingard, C.; Räz, M.; Oka, R.; Manders, F.; Boxtel, R. van; ... ; Sturla, S.J.

DNA Repair 142 (2024) 103755

Contents lists available at ScienceDirect

DNA Repair

journal homepage: www.elsevier.com/locate/dnarepair

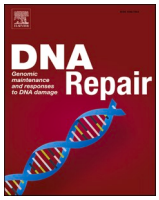

DNA mismatch repair controls the mutagenicity of Polymerase ζ-dependent translesion synthesis at methylated guanines

Anastasia Tsaalbi-Shtylik [a], Cécile Mingard [b], Michael Räz [b], Rurika Oka [c], Freek Manders [c], Ruben Van Boxtel [c], Niels De Wind [a,*], Shana J. Sturla [b,*]

[a] Department of Human Genetics, Leiden University Medical Center, Leiden 2333AL, the Netherlands
[b] Department of Health Sciences and Technology, ETH Zürich, Zürich, 8092, Switzerland
[c] Princess Máxima Center for Pediatric Oncology, Oncode Institute, Utrecht, 3584CS, the Netherlands

ARTICLE INFO

Keywords:
DNA translesion synthesis
DNA polymerase ζ
DNA mismatch repair
O^6-methyldeoxyguanosine
Mutagenesis
Mutational signatures

ABSTRACT

By replicating damaged nucleotides, error-prone DNA translesion synthesis (TLS) enables the completion of replication, albeit at the expense of fidelity. TLS of helix-distorting DNA lesions, that usually have reduced capacity of basepairing, comprises insertion opposite the lesion followed by extension, the latter in particular by polymerase ζ (Pol ζ). However, little is known about involvement of Pol ζ in TLS of non- or poorly-distorting, but miscoding, lesions such as O^6-methyldeoxyguanosine (O^6-medG). Using purified Pol ζ we describe that the enzyme can misincorporate thymidine opposite O^6-medG and efficiently extend from terminal mismatches, suggesting its involvement in the mutagenicity of O^6-medG. Surprisingly, O6-medG lesions induced by the methylating agent *N*-methyl-*N'*-nitro-*N*-nitrosoguanidine (MNNG) appeared more, rather than less, mutagenic in Pol ζ-deficient mouse embryonic fibroblasts (MEFs) than in wild type MEFs. This suggested that *in vivo* Pol ζ participates in non-mutagenic TLS of O^6-medG. However, we found that the Pol ζ-dependent misinsertions at O^6-medG lesions are efficiently corrected by DNA mismatch repair (MMR), which masks the error-proneness of Pol ζ. We also found that the MNNG-induced mutational signature is determined by the adduct spectrum, and modulated by MMR. The signature mimicked single base substitution signature 11 in the catalogue of somatic mutations in cancer, associated with treatment with the methylating drug temozolomide. Our results unravel the individual roles of the major contributors to methylating drug-induced mutagenesis. Moreover, these results warrant caution as to the classification of TLS as mutagenic or error-free based on *in vitro* data or on the analysis of mutations induced in MMR-proficient cells.

1. Introductions

DNA replication and repair greatly impact genomic stability in the presence of genotoxic exposures from endogenous sources, the environment, diet and drugs [1]. DNA translesion synthesis (TLS) polymerases can incorporate opposite and beyond chemically altered DNA nucleotides that would otherwise impede replicative DNA synthesis [2]. TLS thereby avoids replication fork collapse, implicating TLS as a mechanism to prevent genome instability and promote survival in response to DNA lesions. However, fidelity of replication is traded off in the process and therefore TLS is believed to be responsible for most nucleotide substitution mutations induced by helix-distorting nucleotide lesions. Amongst the 15 characterized mammalian DNA polymerases [3], the B-family TLS polymerase zeta (Pol ζ) appears to play a unique and crucial role. Thus, unlike all other TLS polymerases, Pol ζ acts in concert with TLS polymerases of the Y family in a switch mechanism where a member from the Y family TLS polymerases inserts (or misinserts) a nucleotide opposite a helix-distorting nucleotide lesion. Subsequently Pol ζ, which lacks a proofreading domain, extends from the misaligned primer to fix the misincorporation [4]. Deficiency of Pol ζ confers embryonic lethality to mice, in support of its relevance for TLS of endogenous helix-distorting nucleotide lesions or other hard-to-replicate sequences [4,5]. In cultured cells, Pol ζ deficiency leads to chromosomal aberrations [6–8] while cells lacking Pol ζ are hypersensitive to, but hypomutable by, helix-distorting DNA lesions [4]. There is limited information, however, concerning the involvement of mammalian Pol ζ in TLS and the mutagenicity of poorly-distorting DNA adducts, including O^6-medG [9,10].

* Corresponding authors.
E-mail addresses: n.de_wind@lumc.nl (N. De Wind), sturlas@ethz.ch (S.J. Sturla).

https://doi.org/10.1016/j.dnarep.2024.103755
Received 5 May 2024; Received in revised form 27 July 2024; Accepted 16 August 2024
Available online 25 August 2024

O^6-medG is a common modification that arises from reactions of DNA with diverse methylating agents, such as endogenous S-adenosyl methionine, amine nitrosation products but also from exogenous S_N1-type agents such as *N*-methyl-*N*-nitrosourea (MNU), *N*-methyl-*N'*-nitro-*N*-nitrosoguanidine (MNNG), and chemotherapeutic drugs such as dacarbazine and temozolomide [2]. Whereas each day ten to thirty O^6-medG adducts arise in a cell due to endogenous processes [11], temozolomide treatment can increase this number to thousands of adducts per cell [12,13]. The direct reversal protein O^6-Methylguanine-methyl transferase (MGMT) removes the methyl group from O^6-medG. However, MGMT functions in a non-catalytic manner resulting in its depletion at high O^6-medG levels, whereas its expression also can be lost by epigenetic silencing [14]. In contrast to severely helix-distorting DNA lesions, that largely or completely have lost coding capacity, O^6-medG adducts have retained basepairing ability, although pairing is ambiguous resulting in the frequent misinsertion of thymidine [15]. Consequently, O^6-medG induces C>T transition mutations [16]. The mutagenicity of O^6-medG is thought to contribute to carcinogenesis by mutating cancer driver genes, and many cancers have been linked to prior exposure to methylating drugs [17,18]. In support, C>T transitions dominate COSMIC SBS (catalogue of somatic mutations. in cancer) signature 11, which is associated with previous temozolomide therapy [19,20].

The adduct spectrum of methylating drugs has been described [21,22] and cellular factors driving the repair and cytotoxicity of O^6-medG are well characterized [14]. However, the role of DNA polymerases, particularly of Pol ζ, in replicative bypass and mutagenic properties of O^6-medG are not as clearly defined. *In vitro,* the combination of replicative Pol δ or TLS Pol η with Pol ζ or Pol κ *in vitro* bypasses O^6-medG lesions efficiently and in an error-free fashion, where yeast Pol δ or η catalyze nucleotide incorporation, and yeast Pol ζ or human Pol κ can extend from a correct O^6-medG-C primer-template terminus [23–25]. In mammalian cells, proficiency of Pol ζ was linked to temozolomide tolerance [9,10], however its potential activity as an extender polymerase in the context of methylation damage or the impact on mutagenicity is not known. In a study using a human cell line lacking individual TLS polymerases, there was no effect of Pol ζ loss on the mutagenicity of O^6-medG embedded in an episomal vector, arguing against its involvement in mutagenic TLS of the lesion [26]. For mammalian Pol ζ in particular, there are few biochemical studies of adduct bypass [27,28], in part due to difficulty in expressing and purifying this four-subunit complex comprised of REV3L (353 kDa) [29], the catalytic subunit, and accessory factors REV7, PolD2 and PolD3 [30]. It appears that efficient Pol ζ function depends on the hydrogen bonding capacities of the nascent base pairs, which suggests that it could well facilitate extension after O^6-medG-T mispairing as a potential basis of C>T transitions [28]. It was also shown, however, that when C is incorporated opposite another common O^6-guanine adduct, O^6-carboxymethylguanine, DNA synthesis is efficiently extended by isolated human Pol ζ, suggesting also a basis for error-free outcomes, at least with this particular adduct [27,31].

Here we aimed to investigate the involvement of mammalian Pol ζ in TLS of O^6-medG and in O^6-medG-induced mutation frequencies and signatures, using a combination of *in vitro* and *in vivo* approaches. Using purified Pol ζ and site-specific O^6-medG-containing linear replication templates, we first characterized the proficiency and fidelity of isolated human Pol ζ in the bypass of O^6-medG and of the extension of matched or mismatched O^6-medG. Its proficiency in incorporating Thymidine opposite O^6-medG, combined with its propensity to extend from this mismatched Thymidine, suggested that Pol ζ participates in mutagenic TLS of these lesions. We then performed whole-genome sequencing in MNNG-exposed cells that either expressed or were deficient in Pol ζ to gain insight on how this process may shape genome-wide mutational signatures *in vivo*. In apparent contradiction to the activity of the isolated enzyme, Pol ζ-mediated TLS of O^6-medG appeared relatively error-free *in vivo*. We tested the hypothesis that MMR may mask the mutagenicity of Pol ζ on O^6-medG in the cells, by additionally disrupting the core MMR gene *Msh2*. Indeed, in the absence of MMR, Pol ζ-mediated TLS at and beyond O^6-medG appeared error-prone, suggesting that MMR operates downstream of Pol ζ to correct its mutagenic role at O^6-medG. Finally, we determined how functional MMR impacts Pol ζ-associated mutational signatures of MNNG exposure in relation with signatures extracted from human cancer genomes. This analysis indicates that methylation damage, mutagenic TLS and MMR deficiency are key drivers of mutagenesis in therapy-resistant glioma. Collectively, our results reveal that MMR can play an important role in suppressing the mutagenicity of TLS at non-distorting nucleotide lesions and warrant caution in classifying TLS as error-prone or error-free based on the activity of isolated enzymes or on experiments in MMR-proficient cells.

2. Materials and methods

2.1. Chemicals and reagents

[γ-^{32}P]ATP was purchased from PerkinElmer Life Sciences. dNTPs were purchased from Invitrogen and Bioconcept. T4 polynucleotide kinase was purchased from Promega. Tris-HCl (pH 7.0 at 25 °C), Tris-HCl (pH 8.0 at 25 °C), NaCl, $MgCl_2$, dithiothreitol (DTT) and glycerol were purchased from Invitrogen. Bovine serum albumin (BSA) was purchased from New England Biolabs. The hDNA Pol ζ four-subunit-complex (REV3, REV7, POLD2, POLD3) was obtained following the procedure of Lee *et al.* [30] using plasmids kindly provided by the Laboratory of Dr. Wei Yang at the National Institutes of Health, Bethesda. Protein expression and purification was performed by Trenzyme GmbH and a Coomassie PAGE gel of the purified protein is shown in [27]. All other reagents were purchased from Sigma Aldrich.

2.2. Oligonucleotides used in the primer extension assays

A 28mer DNA template 3'-ATT ATG CTG AGT GAT ATC CCT CHX DC A-5' was used for primer extension experiments; X = G was purchased from VBC Biotech, and X=O^6-medG was synthesized on a Mermade 4 DNA synthesizer from Bio Automation Corporation with an O^6-medG phosphoramidite from Links Technologies; the strand was PAGE-purified. D indicates T, A or G and H indicates A, T, and C (IUPAC codes). Primers were purchased from VBC Biotech: P_{23} (23mer) 3'-AG AGG GAT ATC ACT CAG CAT AAT-5', which was used for insertion studies, and P_{24} (24mer) 3'-YWG AGG GAT ATC ACT CAG CAT AAT-5' was used for extension studies. Y indicates T or C, and W indicates A or T.

2.3. Pol ζ primer extension assay

Pol ζ was expressed in insect cells, purified and characterized as described previously [27]. T4 polymerase nucleotide kinase and [γ-^{32}P]ATP were used to 5'-end label primer strands. Labeled primers were annealed to templates by heating at 95 °C for 5 min and then allowed to cool slowly to 25 °C. Primer extension reactions for hDNA Pol ζ were carried out in 20 mM Tris-HCl (pH 8.0, 25 °C), 100 mM NaCl, 5 mM $MgCl_2$, 0.5 mM TCEP (pH 7.0, 25 °C), 100 μg/mL BSA and 3 % glycerol. For each reaction, 10 nM 5'-[^{32}P]primer-template DNA and 5 nM hDNA Pol ζ were used. Reactions were initiated by adding 100 μM dNTP to 5'-[^{32}P]primer-template DNA and hDNA Pol ζ in buffer. Reactions were performed for 15 min at 37 °C, and then terminated by adding 10 μL quenching solution (95 % formamide, 20 mM EDTA, 0.05 % xylene cyanol and bromophenol blue). The resulting solution was loaded on a 15 % polymerized acrylamide 7 M urea gel, run for 4 h at 1500 V, and visualized with a phosphorimager (BioRad).

2.4. Pol ζ steady-state kinetics

Steady-state kinetic assays were performed with a pre-annealed

primer-template DNA, as described for the primer extension assays. hDNA Pol ζ (5 nM) was combined with 50 nM 5'-[^{32}P]-primer-template DNA at 37 °C, in a reaction buffer containing 20 mM Tris-HCl (pH 8.0 at 25 °C), 100 mM NaCl, 5 mM $MgCl_2$, 0.5 mM TCEP (pH 7, 25 °C), 100 μg/mL BSA, 3 % glycerol and increasing dNTP concentrations were added. To determine incorporation efficiency opposite O^6-medG or G, varying concentrations of either dCTP or dTTP were added. To determine extension efficiency from X:N termini, increasing concentrations of dGTP were added. Each reaction was performed three times and the duration was optimized such that product band intensities were lower than 20 %. Reactions were terminated at varying time points by removing aliquots of the reaction, and quenching with a solution containing 95 % formamide, 20 mM EDTA, 0.05 % xylene cyanol and bromophenol blue. Resulting solutions were applied to a 15 % polymerized acrylamide 7 M urea gel and run for four hours at 1500 V. Bands were visualized with a phosphorimager (BioRad, Hercules, CA). Band intensity was quantified using Quantity One Software (BioRad). Nucleotide incorporation levels were plotted as a function of dGTP concentration and fit to the Michaelis-Menten equation with SigmaPlot 12 software. From the hyperbolic plots, parameters k_{cat} and K_M were obtained (represented as mean values ± SD) and used to calculate the frequency of mispair extension (f^o_{ext}) for each primer-template pair and the dNTP incorporation frequency (f_{inc}) on the basis of the following equation: f^o_{ext} or $f_{inc} = (k_{cat}/K_M)_{mispaired}/(k_{cat}/K_M)_{paired}$.

2.5. Isolation and culture of MEFs

Wild-type, *Rev3*$^{-/-}$, *Msh2*$^{-/-}$ and *Rev3*$^{-/-}$ *Msh2*$^{-/-}$ mouse embryonic fibroblasts (MEFs) of hybrid 129/Ola and C57BL/6 background originated from embryos of inter-crossed *Rev3*$^{+/-}$ *Msh2*$^{+/-}$ mice [32,33]. Primary MEFs were isolated by trypsinization of finely minced, 13.5-day-old embryos at 37°C for 15 min. MEFs were cultured in MEF medium (Dulbecco's modified Eagle's medium containing 4500 mg/L glucose, GlutaMax, and pyruvate (Invitrogen) supplemented with 10 % foetal calf serum and antibiotics at 37°C and 5 % CO_2). The cells were immortalized by infection with a retroviral vector expressing a short hairpin RNA against mouse p53 [34].

2.6. Cell sensitivity to MNNG

MEFs were pre-conditioned with 40 μM O^6-BenzylGuanine (O^6-BnG, inhibitor of MGMT) in serum-free medium for 2 h and then exposed to increasing concentrations of MNNG, also in the presence of 40 μM O^6-BnG in serum-free medium for 1 h. Immediately after chemical exposure, cells were collected and seeded at clonal density, the first 2 days in the presence of O^6-BnG. Survival was determined by counting emerging clones 14 days later and normalizing to the number of clones in mock-treated control of the corresponding genotype.

2.7. Single clone expansion following MNNG exposure

To study mutagenesis in response to MNNG, the parental polyclonal line of each genotype was seeded at low density, and clones were picked. One clone with stable morphology, growth capacity and karyotype was selected for each genotype: wild-type, *Rev3*$^{-/-}$, *Msh2*$^{-/-}$ and *Rev3*$^{-/-}$ *Msh2*$^{-/-}$. From each clone, $4*10^6$ cells were harvested for DNA isolation to be used as a baseline reference in sequencing. After that, $1.5*10^6$ MEFs of each clone were seeded in P90 dishes for treatment. On the next day, cells were pre-conditioned either with 40 μM O^6-BnG (inhibitor of endogenous MGMT) or vehicle (0.1 % DMSO) in serum free medium for 2 hours, and then exposed respectively either to 0.5 μM MNNG in the presence of 40 μM O^6-BnG or to vehicle (0.2 % DMSO, mock treatment) in serum free medium. After 1 hour, the medium was replaced with fresh growth medium containing, respectively, either 40 μM O^6-BnG (to avoid repair of O^6-medG by MGMT, MNNG treatment) or vehicle (0.1 % DMSO, mock treatment) for 48 h. The cells were allowed to recover for 48 h in growth medium, then cultured for 15 doublings. Then, the cells were seeded again at low density to generate separate subclones. These subclones were picked and their morphology, growth capacity, karyotype and genotype were checked once more. 2–3 subclones per genotype per treatment were expanded and cells were collected again for DNA isolation and sequencing.

2.8. Illumina sequencing library preparation

DNA was isolated from frozen parental clones and MNNG or mock-exposed subclone cell pellets, using QIASympony SP with the QIAsymphony DSP DNA Mini kit. DNA was sequenced from both ends at 30X coverage on the Xten Illumina platform. DNA from wild type and *Rev3*$^{-/-}$ cells was sequenced by the Hartwig Medical Foundation (Amsterdam), and *Msh2*$^{-/-}$ and *Rev3*$^{-/-}$ *Msh2*$^{-/-}$ by GenomeScan (Leiden).

2.9. Variant calling

Sequence reads were aligned to the mouse reference genome (mm10) using BWA (v0.7.5a).[35] Sam files were converted into bam files and duplicates were removed with Sambamba (v0.6.8).[36] Variants were called for each sample using GATK (v3.4–46) [37] with HaplotypeCaller. The quality of the variants was evaluated using GATK VariantFiltration with the following options: '-snpFilterName LowQualityDepth -snpFilterExpression "QD < 2.0" -snpFilterName MappingQuality -snpFilterExpression "MQ < 40.0" -snpFilterName StrandBias -snpFilterExpression "FS > 60.0" -snpFilterName HaplotypeScoreHigh -snpFilterExpression "HaplotypeScore > 13.0" -snpFilterName MQRankSumLow -snpFilterExpression "MQRankSum < −12.5" -snpFilterName ReadPosRankSumLow -snpFilterExpression "ReadPosRankSum < −8.0" -cluster 3 -window 35'. Full pipeline description and settings are available at https://github.com/UMCUGenetics/IAP (Version 2.6.0) and https://github.com/ToolsVanBox/NF-IAP (Version 1.3.0).

2.10. Single-base substitution filtering

Raw single nucleotide variants were extracted and filtered as previously described [38]. Single-nucleotide variants were filtered based on quality scores values (QUAL >= 100, MQ >= 60, VAF >= 0.1, Coverage >= 20, GQ >= 10 for control sample, GQ >= 99 for treated samples). Mutations were filtered against the parental clone to remove point mutations present in the cell lines before the start of the experiment. Additionally, only unique point mutations among cell line conditions were kept for the final single-base substitution analysis. The scripts are available at https://github.com/ToolsVanBox/SNVFI (Version 1.2). All the subsequent mutation analysis were performed using the R package MutationalPatterns [39].

In order to quantitatively compare mutation frequencies between mock- and MNNG-treated cells, we accounted for any differences in mutation calling efficiencies by normalizing the frequencies of C>T transitions, which were the main outcome of MNNG exposure, to the frequencies of background substitutions at A.T base pairs in each individual genotype. In addition, we corrected for differences in ploidy of each subclone of each genotype by calculating mutation frequencies on a per diploid genome basis for all sequences, and then subtracted the mutations in mock-treated cells from MNNG-treated in order to determine MNNG-induced mutation number and spectrum in each genotype.

2.11. Statistical analysis

Unpaired two-tailed t-tests were performed between biological replicates when n≥3. The Chi-square test was used to determine differences in trinucleotide mutation signatures.

3. Results

3.1. Catalysis of DNA synthesis beyond O^6-MedG by purified DNA Pol ζ

It was shown previously that extension of DNA synthesis from the C in a terminal O^6-medG:C is catalyzed by purified human DNA Pol ζ heterotetrameric holoenzyme, and that the efficiency of this process is influenced by H-bonding interactions at the DNA primer terminus [28], yet its proficiency to either misincorporate at the adduct or catalyze DNA synthesis extension after a nucleotide other than C is misincorporated, was not examined. Thus, we here performed primer extension assays to determine the fidelity of nucleotide insertion by Pol ζ opposite O^6-medG, as well as the efficiency of subsequent extension. To address the question of insertion, we used 28-mer DNA templates with G or O^6-medG at position 24 (from the 3' end) of the template annealed to a 23-mer primer (Fig. 1A). When the template had O^6-medG, misinsertion of dTTP was favored 1,600-fold over dCTP, compared with a 2,900-fold preference of the correct substrate dCTP over dTTP when the template had G (Table 1). Purine insertion was too low to quantify. These data suggest Pol ζ to have mutagenic potential as an error-prone inserter at O^6-medG.

Since Pol ζ acts as an extender during TLS of helix-distorting lesions, we then tested extension by Pol ζ from 3'-terminal matched (C) or mismatched (T) nucleotides opposite O^6-medG or G, by using 24-mer primers with different matched or mismatched canonical bases opposite the O^6-medG or G (Fig. 1B). The frequency of mismatch extension (f°_{ext}), normalized to k_{cat}/K_M values for extension, was highest when the substrate contained a terminal O^6-medG:T mismatch (k_{cat}/K_M of 0.40 $\mu M^{-1}min^{-1}$, Table 2, Entry 4).

Remarkably, this extension was four-fold more efficient than extension from G:C (k_{cat}/K_M of 0.10 $\mu M^{-1}min^{-1}$, Table 2, entry 1), attributable to a relatively favorable K_M for O^6-medG (0.38 μM, Table 2). Furthermore, the extension frequency was low when O^6-medG was mispaired with A or G (Table 2, entries 5–8), as judged by the lack of G>T and G>C transversions (see also below). Thus, by misincorporating thymidine opposite O^6-medG by either Pol ζ or another polymerase, followed by Pol ζ-mediated extension from the mismatched nucleotide pair, Pol ζ could be active in mutagenic TLS of these non-helix-distorting lesions.

To understand whether the DNA sequence context might influence the potential for extension of a terminal O^6-medG:T mismatch by Pol ζ to cause C>T transitions, we evaluated the impact of identity of bases flanking O^6-medG on extension efficiencies. Using the same oligonucleotide templates as the experiment above, but varying only the bases that flank O^6-medG with purines, pyrimidines or both, we compared extension from O^6-medG:T vs. O^6-medG:C, as well as from G:T vs. G:C. Extension from O^6-medG:T was more efficient than from O^6-medG:C in the T(O^6-medG)A, and especially, the T(O^6-medG):C context, and the preference and magnitude varied considerably amongst the sequence contexts (Fig. 2 A).

For the unmodified controls, on the other hand, extension of Pol ζ from G:C was more efficient than from the mismatch G:T in all tested contexts (Fig. 2B). Collectively, these data are consistent with the potential for mutations to arise by a polymerase switch model [4,40] in which Pol ζ either misinserts T and then extends, or it extends after another polymerase misinserts T opposite O^6-medG, particularly in

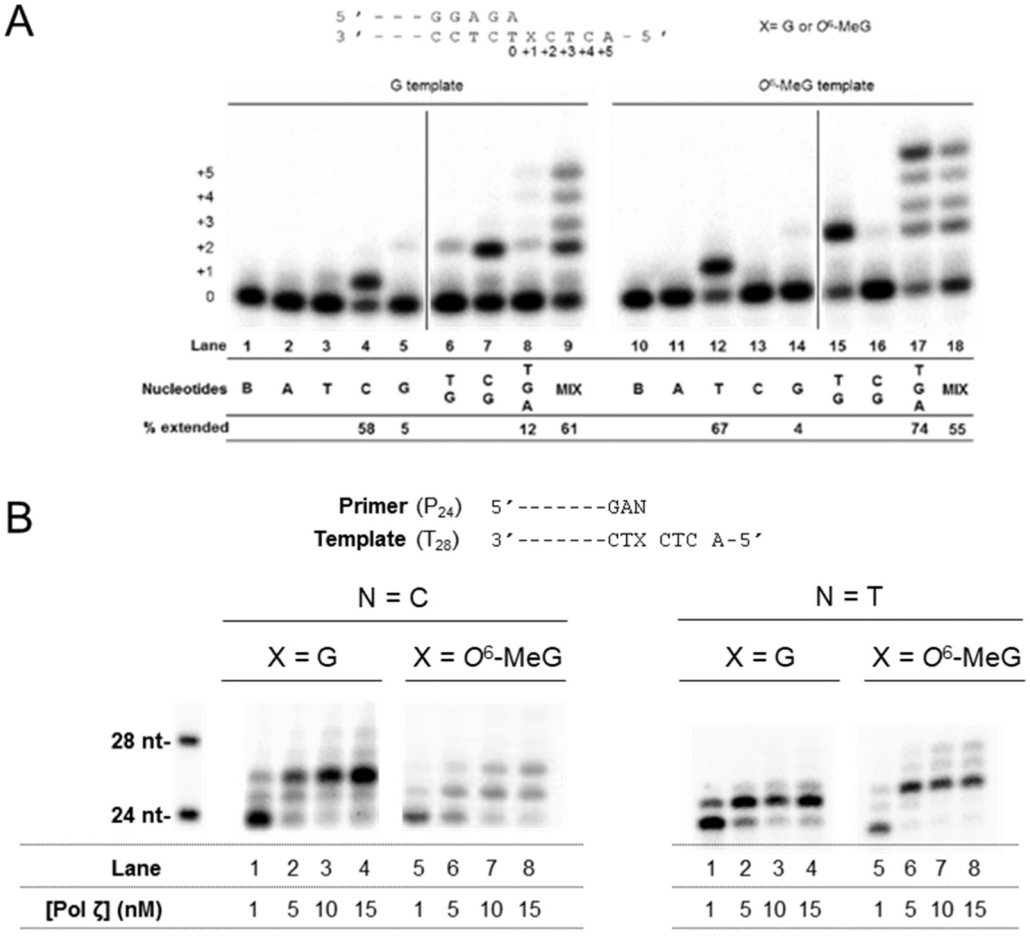

Fig. 1. Primer-extension assay for (A) incorporation opposite G vs. O^6-medG. Nucleotides: B, Blank; A, dATP; T, dTTP; C, dCTP; G, dGTP; Mix, all four dNTPs. (B) extension from C or T placed opposite G vs. O^6-medG with increasing concentrations of hPol ζ. Representative images from three replicate experiments shown.

Table 1
Steady-state kinetics for incorporation by hDNA Pol ζ of dCTP or dTTP opposite G or O^6-medG.

Entry	Template	dNTP	K_M [μM]	k_{cat} [min^{-1}]	k_{cat}/K_M [$\mu M^{-1}min^{-1}$]	f_{inc}	Preferred dNTP
1	G	dCTP	3.1±0.6	0.14	4.4×10^{-2}	1.0	dCTP>>dTTP ~2900 fold
2		dTTP	325±112	0.0050	1.5×10^{-5}	0.0003	
3	O^6-medG	dCTP	185±54	0.0030	1.5×10^{-5}	0.0003	dTTP>>dCTP ~1600 fold
4		dTTP	5.9±1.1	0.14	2.4×10^{-2}	0.55	

Table 2
Steady-state kinetics for incorporation by hDNA Pol ζ of dGTP after the indicated basepair or mispair by hDNA Pol ζ.

Entry	primer: template	KM [μM]	kcat [min-1]	kcat/KM [μM-1 min-1]	f[a]exta
1	G:C	1.8 ± 0.50	0.18	1.0 ×10–1	1.0
2	O6-medG:C	8.7 ± 2.4	0.24	2.7 ×10–2	0.28
3	G:T	17 ± 5.2	0.26	1.6 ×10–2	0.15
4	O6-medG:T	0.38 ± 0.05	0.15	4.0 ×10–1	4.0
5	G:A	31 ± 8.0	0.25	8.0 ×10–3	0.08
6	O6-medG:A	15 ± 3.7	0.26	1.7 ×10–2	0.18
7	G:G	34 ± 9.2	0.20	6.0 ×10–3	0.06
8	O6-medG:G	38 ± 8.9	0.19	5.0 ×10–3	0.05

[a] $f_{ext} = (k_{cat}/K_M)_{mispaired}/(k_{cat}/K_M)_{paired}$

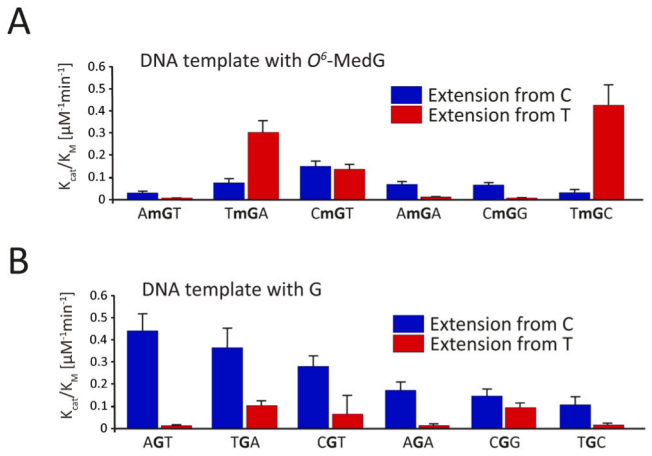

Fig. 2. (A) Michaelis-Menten parameters for DNA extension synthesis from O^6-medG:C or O^6-medG:T (mis)pairing in different trinucleotide contexts by purified hDNA Pol ζ. (B) Michaelis-Menten parameters for DNA extension synthesis by hDNA Pol ζ from a G:C or G:T terminus in different trinucleotide contexts. Data represent the mean of three independent experiments +/- SD.

certain contexts.

3.2. *in vivo, Pol ζ appears error-free during TLS of O^6-medG*

Rev3-deficient cells are sensitive to the methylating agent MNNG and temozolomide [10]. By exposing MEFs (wild type vs. *Rev3*$^{-/-}$) to increasing MNNG concentrations in the presence of the MGMT inhibitor O^6-Benzylguanine (O^6-BnG) to prevent reversal of O^6-medG, we confirmed this sensitivity to MNNG-induced methylation (Supplementary Figure 1). Next, we used these cells to test the impact of Pol ζ on the mutagenicity of MNNG *in vivo*. Independent subclones of wild type and *Rev3*$^{-/-}$ MEF lines were isolated and these were either mock-treated or exposed to MNNG in the presence of O^6-BnG, and expanded for 15 generations to fix the mutations, thereby taking into account the differences in growth between the lines. O^6-medG comprises only 8 % of the total DNA methylation damage from MNNG, but the high mutagenic potency of O^6-medG and the sole induction of C>T transitions in cells suggests that virtually all MNNG-induced mutations result from mispairing of O^6-medG with Thymidine. After expansion, we subcloned the cells again (2–3 subclones per genotype and per treatment) and performed whole-genomic sequencing of the parental subclones and of each treated subclone (Fig. 3 A). This procedure allowed us to filter out preexisting and spontaneous mutations and thus identify the MNNG-induced mutations. To enable to quantitatively compare the frequencies of MNNG-induced mutations within each genotype, mutation frequencies within mock- or MNNG-treated cells were normalized within each genotype to the number of mutated A:T base pairs. The latter mutations are refractory to mutagenesis by MNNG and therefore can serve as internal standards, enabling to correct for differences in the efficiency of variant calling. We also corrected for differences in ploidy of the lines (Supplementary Figure 2), thus defining the number of C>T transitions on the basis of a diploid genome. In addition we subtracted the mutations in mock-treated cells from MNNG-treated cells in order to determine MNNG-induced mutation numbers and spectra in each genotype.

In apparent contradiction with the primer extension experiments, Pol ζ-deficiency resulted in a significant (p=0.01) 3.5-fold increase of the frequency of MNNG-induced nucleotide substitutions *in vivo* (Fig. 3B). This increased mutagenicity might suggest that Pol ζ may act in a relatively error-free TLS pathway at O^6-medG *in vivo*. In addition, the increased mutagenicity of MNNG in the absence of Pol ζ implies the existence of a redundant inserter and/or extender polymerase that is more mutagenic than Pol ζ. MNNG uniquely induced C>T transitions in both genotypes, confirming the notion that O^6-medG is the only mutagenic lesion induced by the drug, irrespective of the Pol ζ status (Fig. 3 C).

3.3. *Mismatch repair corrects Pol ζ-associated misincorporations at O^6-medG*

Considering the discrepancy between the mutagenic insertion and extension from O^6-medG:T by isolated Pol ζ and the relatively error-free role of Pol ζ in MNNG-induced mutagenesis in cells, we hypothesized that additional factors control Pol ζ-dependent mutations at O^6-medG *in vivo*. DNA mismatch repair (MMR) was a prime candidate as it suppresses the mutagenicity of methylating agents [41]. This possibility was not obvious since in *S. cerevisiae* MMR does not operate downstream of Pol ζ [42,43] and, in contrast to mammalian cells, MMR does not mediate the cytotoxicity of methylating drugs in *S. cerevisiae* [44]. To investigate a role for MMR in correcting Pol ζ-dependent mutagenic TLS at O^6-medG in the mammalian context, we generated isogenic MMR-deficient (*Msh2*$^{-/-}$) and Pol ζ+MMR (*Rev3*$^{-/-}$*Msh2*$^{-/-}$) double-deficient MEF lines. We first investigated the toxicity of MNNG in these cell lines, in the presence of O^6-BnG. In Pol ζ-proficient cells MMR mediated the toxicity of MNNG, reflecting the lethal processing of O^6-medG:T mispairs by MMR (Supplementary Figure 3). However, in the absence of Pol ζ, MMR deficiency rescued the toxicity of MNNG to a lower extent. This result might suggest that, in the absence of Pol ζ, less O^6-medG:T mispairs are produced that kill the cells in an MMR-dependent fashion. This result would be consistent with a mutagenic role for Pol ζ during TLS of O^6-medG also *in vivo* (see below). Of note, the increased sensitivity of *Rev3*$^{-/-}$*Msh2*$^{-/-}$ MEFs, compared with *Msh2*$^{-/-}$ MEFs, may reflect a role of Pol ζ in TLS of the 92 % of MNNG-induced lesions other than O^6-medG.

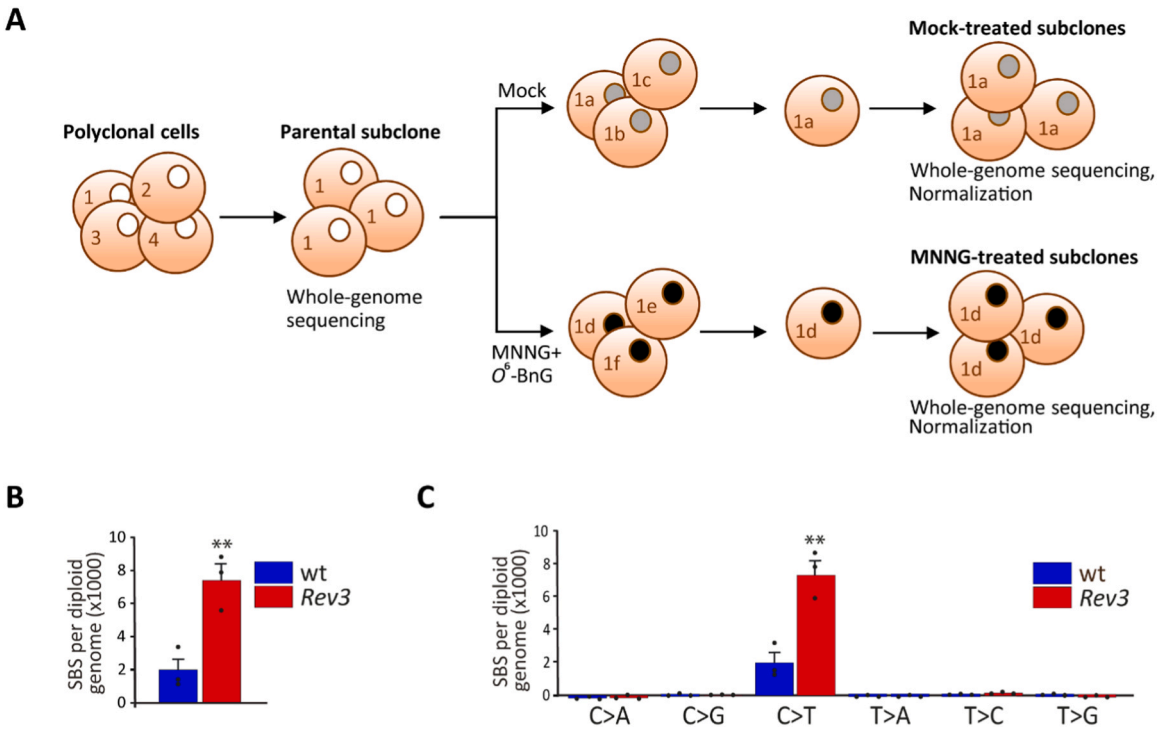

Fig. 3. (A) Experimental design of exposures and clonal expansion. Population containing cells with different number represent multiclonal cell lines, population with the same number represent parental clonal lines and populations with the same number and letter represent experimental subclonal lines. (B) Normalized mutation number induced by MNNG per diploid genome for wild type and *Rev3*$^{-/-}$ cells. (C) Normalized numbers of all possible SBS induced by MNNG per diploid genome for wild type and *Rev3*$^{-/-}$ cells. Data represent the data of three independent experiments +/- SD. Unpaired t-test; **p-value < 0.01.

Using these MEF lines we then repeated the MNNG-treatment and whole genome sequencing experiments. In Pol ζ-proficient cells, MMR suppressed the mutagenicity of MNNG by approximately 70-fold (compare the green bars from Fig. 3B and Fig. 4 A), which implies the efficient correction of misincorporations at O^6-medG. Meanwhile, in Pol ζ-deficient cells, MMR suppressed the mutagenicity of MNNG only 15-fold (compare the red bars from Fig. 3B and Fig. 4 A). In fact, in the absence of MMR, loss of in Pol ζ resulted in a slight (but non-significant) decrease in MNNG-induced mutations, consistent with error-prone activity of Pol ζ that only becomes evident in the absence of MMR (Fig. 4 A). In all cells, the SBS profiles again were dominated by C>T transitions, in agreement with the causal role of O^6-medG of these transition mutations (Fig. 4B). We conclude that MMR suppresses the mutagenicity of Pol ζ-independent and, even more efficiently, of Pol ζ-dependent C>T mutagenesis at O^6-medG. This notion would imply that Pol ζ-dependent TLS at O^6-medG in fact is mutagenic also *in vivo* but that this mutagenicity is suppressed efficiently by MMR. Moreover, this result is consistent with the stronger rescue of MNNG toxicity by disrupting MMR in Pol ζ-proficient MEFs than in Pol ζ-deficient MEFs where less O^6-medG:T mispairs are produced (Supplementary Figure 3). Of relevance, in *Msh2*$^{-/-}$ MEFs but not in wild type MEFs, MNNG also induced double base substitutions (DBS), mainly CN>NN (Fig. 4 C) with half being CC>TT transitions (Supplementary Figure 4). These DBS completely depended on Pol ζ as they were virtually absent in the *Rev3*$^{-/-}$ and in the *Rev3*$^{-/-}$*Msh2*$^{-/-}$ MEFs. This result corroborates the propensity of Pol ζ to produce tandem substitutions at endogenous non-distorting DNA lesions [45] and can best be explained by the Pol ζ-dependent TLS of O^6-medG to produce tandem misincorporations, and their subsequent efficient repair by MMR. Collectively, our results suggest that, in mammalian cells, the sequential activity of Pol ζ and MMR promotes the low mutagenicity of nucleotide lesions that have retained coding capacity.

3.4. *Mutational signatures of MNNG-exposed MEFs reflect the adduct signature and are modulated by MMR, but not by TLS*

With whole genome sequencing data at hand, we looked more closely into the relative frequencies of MNNG-induced single base substitutions within all trinucleotide contexts in relation to Pol ζ and to MMR deficiency, alone or in combination. In MMR-proficient cells, disruption of Pol ζ led to an increase of the frequency of MNNG-induced C>T transitions in most trinucleotide contexts (Fig. 5A), underscoring the (apparently) error-free function of Pol ζ in TLS in the presence of MMR. Irrespective of the Pol ζ status, guanines flanked with a 5' purine

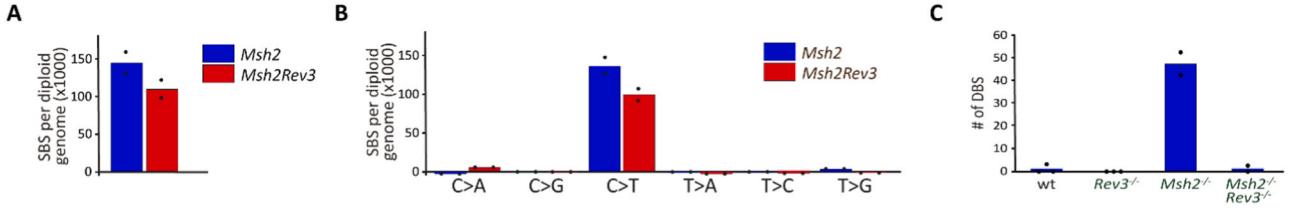

Fig. 4. (A) Normalized numbers of mutations induced by MNNG per diploid genome for *Msh2*$^{-/-}$ and *Msh2*$^{-/-}$*Rev3*$^{-/-}$ cells. (B) Normalized numbers and type of mutations induced by MNNG per diploid genome for *Msh2*$^{-/-}$ and *Msh2*$^{-/-}$*Rev3*$^{-/-}$ *cells*. (C) Tandem substitutions per diploid genome induced by MNNG for all four genotypes. Data represent the data of at least two independent experiments.

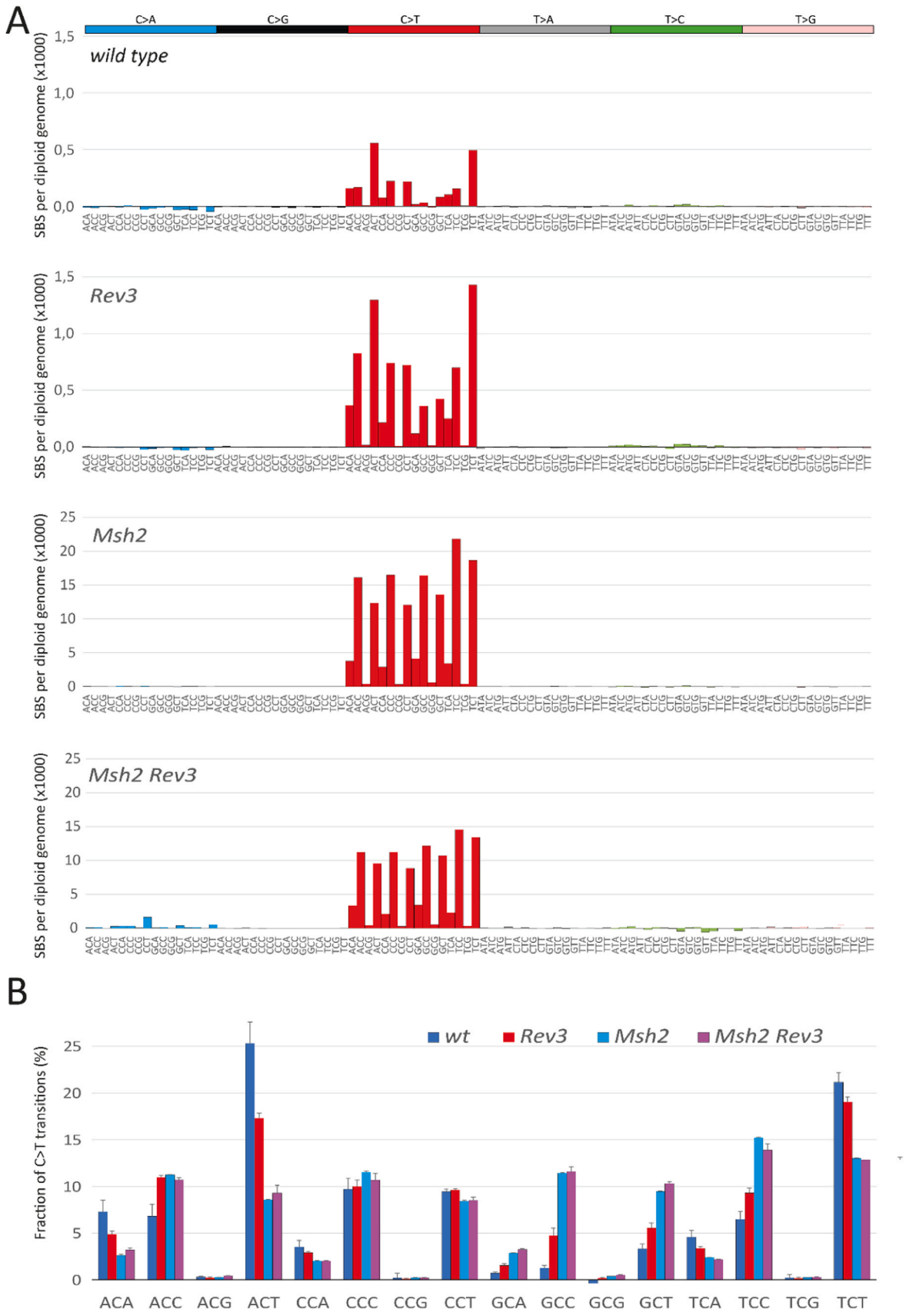

Fig. 5. A: Normalized frequencies of the six base substitutions in a trinucleotide context, induced by MNNG in *wild type, Rev3*$^{-/-}$, *Msh2*$^{-/-}$ and *Msh2*$^{-/-}$*Rev3*$^{-/-}$ MEFs. B: Relative frequencies of MNNG-induced C>T transitions in the 16 possible trinucleotides in all four genotypes.

were particularly prone to undergo MNNG-induced C>T transitions. This preference reflects the sequence preference of guanine methylation, i.e. a template purine 5' of the G [21,22].

Like in the MMR-proficient cells, the MNNG-induced trinucleotide mutation signature in MMR-deficient cells was independent of the Pol ζ status. This underscores the irrelevance for the eventual mutational outcomes on whether Pol ζ or a redundant polymerase has acted during mutagenic TLS of O^6-medG (Figs. 5A, 5B). However, we observed a significant difference in the relative trinucleotide distribution of substitutions between wild type and *Msh2*$^{-/-}$ cells (Chi^2 p=0.004) and between wild type and *Rev3*$^{-/-}$*Msh2*$^{-/-}$ cells (Chi^2 p=0.009; Fig. 5B). On the other hand, the distribution was similar between wild type and *Rev3*$^{-/-}$ cells (Chi^{i2} p=0.998) and in both MMR-deficient groups *Msh2*$^{-/-}$ and *Rev3*$^{-/-}$*Msh2*$^{-/-}$ (Chi^2 p=1.000). Thus, in the absence of MMR not only A(O^6-medG)T and A(O^6-medG)A, but all trinucleotides with a template purine 5' of the O^6-medG were approximately equally prone to originate C>T transitions.

This indicates that MMR corrects misincorporations of thymidine at A(O^6-medG)T and A(O^6-medG)A trinucleotides less efficiently than in other trinucleotides, irrespective of their origin. Moreover, the MNNG-induced mutation signatures in the absence of MMR (Fig. 5) poorly correlated with the *in vitro* efficiency of extension from O^6-medG:T by Pol ζ (Fig. 2 A, Table 3). Therefore, we conclude that MNNG-induced mutational signature is determined by the purine-G methylation preference of MNNG, rather than by the inserter or the extender polymerases. This signature then is modulated by differential MMR (Fig. 5B).

3.5. Mutational signatures of MNNG-exposed MEFs share characteristics of cancer mutational signatures

We further expanded our analysis to compare, on the basis of cosine similarity, the high-resolution mutational spectra of MNNG-treated cells with mutational signatures extracted by non-negative matrix factorization from human cancer genomes (COSMIC signatures; Fig. 6) [19]. Three previously annotated signatures had a cosine similarity greater than 0.80 (arbitrary cut-off between low and high similarity between signatures) with at least one of the newly characterized genomes. All trinucleotide mutational spectra in MNNG-treated cells of all genotypes were highly similar to Signature 11 (cosine similarities 0.90–0.98), with *Msh2*$^{-/-}$ and *Rev3*$^{-/-}$ *Msh2*$^{-/-}$ being almost identical to it (cosine similarity close to 1; cosine similarity analysis does not allow generation of p values). Signature 11 has been attributed to treatment of cancer patients with temozolomide in the context of MMR deficiency. The spectra of the MMR-deficient cell lines were also similar to signature 23 (cosine similarity 0.81), which is thought to arise from guanine alkylation [20,46], and the spectra from wild type and Pol ζ-deficient cells were similar to signature 32 (cosine similarity 0.86), which has been attributed to azathioprine, an immunosuppressant drug that leads to the incorporation of S^6-medG in genomic DNA [19]. The pervasive and strong similarity with Signature 11, in particular in both contexts lacking MMR, is consistent with the profile reflecting an intrinsic mutation profile induced by O^6-medG. Moreover, it supports the etiological influence of either reduced MMR function or saturation of MMR capacity in the etiology of secondary cancers arising after temozolomide therapy, as the MMR defect leaves unrepaired replication errors resulting from misincorporations by TLS opposite methylated nucleotides.

4. Discussion

The concerted influences of DNA damage, DNA repair and TLS shape landscapes of mutations that accumulate in cancer genomes. The individual contributions of these mechanisms to mutation frequencies and signatures are exceedingly difficult to unravel. Here we have addressed this conundrum by combining *in vitro* primer extension experiments using purified Pol ζ with *in vivo* experiments using cells with defects in MGMT, and in TLS or MMR, alone or in combination. Results of our experiments with purified mammalian heterotetrameric Pol ζ holoenzyme suggested that Pol ζ, while its capacity to correctly insert opposite the lesion was poor, could promote the accumulation of mutations due to its proficiency in inserting a thymidine opposite an O^6-medG adduct, and then extending from the mismatch. Alternatively, Pol ζ may extend from a thymidine, misincorporated by another polymerase opposite O^6-medG. Regardless of the identity of the inserter polymerase, a high preference for pairing of T with O^6-medG is consistent with the H-bond-acceptor-donor-acceptor profile for T. This arrangement leads to a C>T transition and is consistent with data obtained using the yeast heterodimeric Rev3/Rev7 core enzyme [23,24].

Disruption of Pol ζ in human cells does not affect the mutagenicity of O^6-medG in a transfected plasmid [26]. Nevertheless we found that cells lacking Pol ζ unexpectedly showed elevated, rather than reduced, mutagenesis. This seemed to suggest that in the chromosomal context Pol ζ may actually operate in a relatively error-free fashion during TLS at O^6-medG in cells while, in its absence, a redundant and more error-prone polymerase(s) takes over. While the replicative pol δ can incorporate opposite O^6-medG, Pol η and Pol κ are candidates for such extender polymerases [24,25,47].

The discrepancy between the mutagenic activity of purified Pol ζ and its apparent error-free nature in cells led us to hypothesize that another mechanism, absent in the biochemical assay, might specifically suppress Pol ζ-dependent mutagenesis at O^6-medG. Indeed, we found that MMR strongly mitigated the Pol ζ-dependent mutagenicity of O^6-medG. The suppression of mutagenesis by MMR varied with the sequence context. In addition, the results were consistent with MMR having less of an impact on mutations arising from the action of alternative polymerase (s). This differential activity might be related to the fact that Pol ζ is a B type polymerase while Pol η and Pol κ are of the Y type. The induction of Polζ-dependent double substitutions by MNNG, at and beyond O^6-medG, and their complete repair by MMR provided additional evidence for this conclusion (Fig. 4 C). Thus, the combined activity of (error-prone) Pol ζ-dependent TLS and the strong suppression of its mutagenicity by MMR provides an effective mechanism to minimize the mutagenicity of these non-distorting lesions. The MMR-mediated

Table 3
Comparison between enzymatic extension from a O^6-medG:T mismatch in different trinucleotides with corresponding mutational frequencies in MNNG-exposed cells.

Trinucleotide context	Extension rate for isolated enzyme[a]	Relative extension rate for isolated enzyme	SBS frequencies in MMR-deficient cells[b]	Relative SBS frequencies in MMR-deficient cells	SBS:enzyme ratio[c]
AmGT/ACT	0.005	1	12.3	41.0	41.0
TmGA/TCA	0.3	60	3.4	11.3	0.2
CmGT/ACG	0.15	30	0.4	1.3	0.04
AmGA/TCT	0.01	2	18.6	62.0	31.0
CmGG/CCG	0.005	1	0.3	1.0	1.0
TmGC/GCA	0.45	90	4.1	13.7	0.2

[a] Kcat/Km [$\mu M^{-1}min^{-1}$]. Derived from Fig. 2 A.
[b] *Msh2*$^{-/-}$ cells; x10^3. Derived from Fig. 5A.
[c] The cell:enzyme ratio reflects the MNNG-induced relative SBS frequency in *Msh2*$^{-/-}$ cells, divided by the relative extension rate for isolated Pol ζ, to reflect the discrepancy between biochemical and *in vivo* (SBS) data.

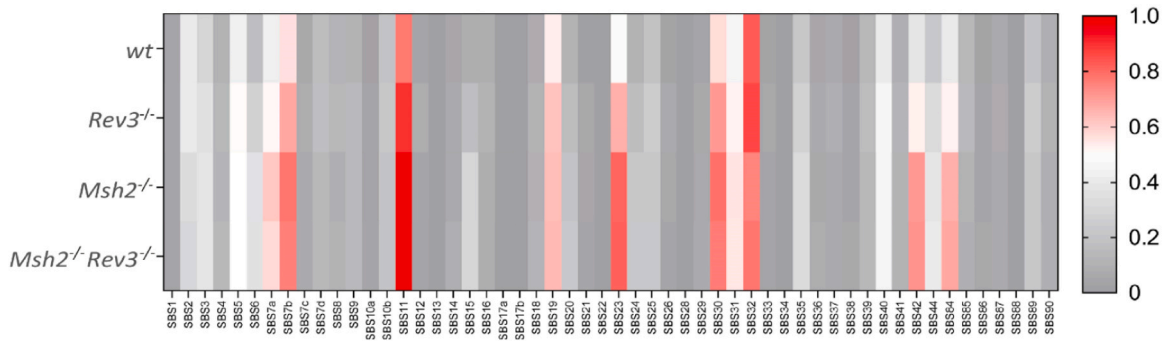

Fig. 6. Cosine similarity of mutational spectra with previously annotated COSMIC mutational signatures.

correction of Pol ζ-dependent mutagenic TLS products reveals a fundamental difference in MMR between lower and higher eukaryotes as in *S. cerevisiae* MMR does not operate efficiently downstream of Pol ζ [42,43]. In agreement, unlike in mammalian cells, in *S. cerevisiae*, MMR does not mediate the cytotoxicity of methylating drugs [44], which is believed to depend on the excision of misincorporations opposite O^6-medG.

Although our experiments using purified Pol ζ suggested a role of the polymerase as a mutagenic inserter and extender at non-distorting lesions, the efficiency of mutagenic TLS by the purified protein at specific trinucleotides compared to MNNG-induced mutational spectra in cells are not consistent. This indicates that misincorporation ratios derived from *in vitro* TLS experiments can be poor predictors of the mutagenic phenotype resulting from the function of a TLS polymerase in a cell. We note that in MMR-deficient cells, irrespective of their Pol ζ status, MNNG-induced mutational signatures are consistent with the O^6-medG adduct preference (Purine preceding G) [21,22]. We hypothesize that, rather than the nature of the inserter polymerase, the physicochemical properties of the O^6-medG in the template determines the nature of the nucleotide (dT or dC) that is (mis)incorporated. Pol ζ, however, may be exquisitely capable of extending from a misincorporated nucleotide, explaining its propensity to 'fixate' such a misincorporation and explaining its mutagenicity, at least in the absence of MMR. In MMR-proficient cells, this repair pathway may then preferentially repair Pol ζ-extended misincorporations, albeit in a mildly sequence context-biased fashion (Fig. 5B). Our data furthermore imply that the MEF cell model used here is well suited for delineating the individual roles of Pol ζ and MMR in determining the mutagenic outcomes of exposure to DNA-damaging chemicals.

When comparing the high-resolution mutational signatures induced by MNNG with human cancer mutational signatures, we found that all MNNG-induced mutations, in particular in *Msh2*$^{-/-}$ and in *Rev3*$^{-/-}$*Msh2*$^{-/-}$ cells, were almost identical to mutational Signature 11, which is annotated as arising from exposure to the methylating drug temozolomide [18,20], in particular in MMR-deficient gliomas [46,48]. Thus, in these gliomas, temozolomide exposure might have selected for drug-resistant, MMR-deficient cells. This gives rise to Signature 11, consequent to the Pol ζ-dependent and -independent mutagenesis mechanism delineated above.

The evidence provided here that MMR suppresses most of the Pol ζ-dependent misincorporations at O^6-medG, implies that MMR plays an important function in the control of mutagenic TLS at non-helix-distorting DNA adducts, that retain some form of basepairing. Indeed, MMR has also been proposed to repair mismatches at poorly-distorting 8-oxoguanines and uracils (reviewed in [49,50]). This non-canonical function of MMR might possibly be extended to DNA lesions with intermediate coding capacity. Thus, we have previously found that MMR also suppresses the TLS-dependent mutagenicity of UV-induced, moderately helix-distorting, cyclobutane pyrimidine dimers [51]. Collectively, our findings reveal a new layer of interaction between mutagenic TLS and anti-mutagenic MMR to control mutagenic and DNA damage responses to unrepaired DNA lesions. Finally, the activity of this dual control mechanism warrants caution as to the interpretation of data on the involvement and mutagenicity of TLS polymerases in the bypass of endogenous or exogenous DNA lesions, when MMR is active.

Accession numbers

Whole genome sequencing data (bam files) are deposited in the European Nucleotide Archive (ENA), ENA Browser (ebi.ac.uk), accession number PRJEB53613. The VCF files can be found in Zenodo: https://doi.org/10.5281/zenodo.8233434

Funding

This work was supported by the Swiss National Science Foundation (185020 and 186332 to S.J.S.), National Institutes of Health [AA123456 to A.B., BB123456 to C.D.; and the Alcohol & Education Research Council [abcde123456]. A.T-S was funded by Dutch Cancer Society grant 11358 awarded to NdW.

Declaration of Competing Interest

The authors declare that they have no known competing financial interests or personal relationships that could have appeared to influence the work reported in this paper.

Data Availability

WGS (bam files) deposited in the European Nucleotide Archive (ENA) with accession number PRJEB53613. VCF files in Zenodo: https://doi.org/10.5281/zenodo.8233434

Acknowledgement

We thank Professor Maureen Mckeague for valuable scientific discussions, Jacob G. Jansen for discussions, technical assistance and critical review of the manuscript, and Lemelinda Marques for performing the *Rev3* and *Msh2* genotyping.

Supplementary data

Supplementary Data are available at DNA Repair online.

Appendix A. Supporting information

Supplementary data associated with this article can be found in the online version at doi:10.1016/j.dnarep.2024.103755.

References

[1] A. Tubbs, A. Nussenzweig, Endogenous DNA damage as a source of genomic instability in cancer, Cell 168 (2017) 644–656.
[2] D. Fu, J.A. Calvo, L.D. Samson, Balancing repair and tolerance of DNA damage caused by alkylating agents, Nat. Rev. Cancer 12 (2012) 104–120.
[3] P.J. Beuning, DNA polymerases: from molecular mechanisms to human disease, a special issue, Chem. Res Toxicol. 30 (2017) 1921.
[4] S.K. Martin, R.D. Wood, DNA polymerase zeta in DNA replication and repair, Nucleic Acids Res 47 (2019) 8348–8361.
[5] B. Ben Yamin, S. Ahmed-Seghir, J. Tomida, E. Despras, C. Pouvelle, A. Yurchenko, J. Goulas, R. Corre, Q. Delacour, N. Droin, P. Dessen, D. Goidin, S.S. Lange, S. Bhetawal, M.T. Mitjavila-Garcia, G. Baldacci, S. Nikolaev, J.C. Cadoret, R. D. Wood, P.L. Kannouche, DNA polymerase zeta contributes to heterochromatin replication to prevent genome instability, EMBO J. 40 (2021) e104543.
[6] S.S. Lange, J. Tomida, K.S. Boulware, S. Bhetawal, R.D. Wood, The polymerase activity of mammalian dNA Pol zeta is specifically required for cell and embryonic viability, PLoS Genet 12 (2016) e1005759.
[7] A. Bhat, P.L. Andersen, Z. Qin, W. Xiao, Rev3, the catalytic subunit of Polzeta, is required for maintaining fragile site stability in human cells, Nucleic Acids Res 41 (2013) 2328–2339.
[8] E. Sonoda, T. Okada, G.Y. Zhao, S. Tateishi, K. Araki, M. Yamaizumi, T. Yagi, N. S. Verkaik, D.C. van Gent, M. Takata, S. Takeda, Multiple roles of Rev3, the catalytic subunit of polzeta in maintaining genome stability in vertebrates, EMBO J. 22 (2003) 3188–3197.
[9] P. Monti, Y. Ciribilli, D. Russo, A. Bisio, C. Perfumo, V. Andreotti, P. Menichini, A. Inga, X. Huang, B. Gold, G. Fronza, Rev1 and Polzeta influence toxicity and mutagenicity of Me-lex, a sequence selective N3-adenine methylating agent, DNA Repair (Amst.) 7 (2008) 431–438.
[10] W.P. Roos, A. Tsaalbi-Shtylik, R. Tsaryk, F. Guvercin, N. de Wind, B. Kaina, The translesion polymerase Rev3L in the tolerance of alkylating anticancer drugs, Mol. Pharm. 76 (2009) 927–934.
[11] B. Rydberg, T. Lindahl, Nonenzymatic methylation of DNA by the intracellular methyl group donor S-adenosyl-L-methionine is a potentially mutagenic reaction, EMBO J. 1 (1982) 211–216.
[12] A. Kraus, M. McKeague, N. Seiwert, G. Nagel, S.M. Geisen, N. Ziegler, I. A. Trantakis, B. Kaina, A.D. Thomas, S.J. Sturla, J. Fahrer, Immunological and mass spectrometry-based approaches to determine thresholds of the mutagenic DNA adduct O6-methylguanine in vivo, Arch. Toxicol. 93 (2019) 559–572.
[13] B. Stratenwerth, S.M. Geisen, Y. He, L. Beltzig, S.J. Sturla, B. Kaina, Molecular dosimetry of temozolomide: quantification of critical lesions, correlation to cell death responses, and threshold doses, Mol. Cancer Ther. 20 (2021) 1789–1799.
[14] P. Bai, T. Fan, G. Sun, X. Wang, L. Zhao, R. Zhong, The dual role of DNA repair protein MGMT in cancer prevention and treatment, DNA Repair (Amst.) 123 (2023) 103449.
[15] J.J. Warren, L.J. Forsberg, L.S. Beese, The structural basis for the mutagenicity of O (6)-methyl-guanine lesions, Proc. Natl. Acad. Sci. USA 103 (2006) 19701–19706.
[16] A. Tomita-Mitchell, L.L. Ling, C.L. Glover, J. Goodluck-Griffith, W.G. Thilly, The mutational spectrum of the HPRT gene from human T cells in vivo shares a significant concordant set of hot spots with MNNG-treated human cells, Cancer Res 63 (2003) 5793–5798.
[17] N. Saini, J.F. Sterling, C.J. Sakofsky, C.K. Giacobone, L.J. Klimczak, A. B. Burkholder, E.P. Malc, P.A. Mieczkowski, D.A. Gordenin, Mutation signatures specific to DNA alkylating agents in yeast and cancers, Nucleic Acids Res 48 (2020) 3692–3707.
[18] J. Wang, E. Cazzato, E. Ladewig, V. Frattini, D.I. Rosenbloom, S. Zairis, F. Abate, Z. Liu, O. Elliott, Y.J. Shin, J.K. Lee, I.H. Lee, W.Y. Park, M. Eoli, A.J. Blumberg, A. Lasorella, D.H. Nam, G. Finocchiaro, A. Iavarone, R. Rabadan, Clonal evolution of glioblastoma under therapy, Nat. Genet 48 (2016) 768–776.
[19] L.B. Alexandrov, J. Kim, N.J. Haradhvala, M.N. Huang, A.W. Tian Ng, Y. Wu, A. Boot, K.R. Covington, D.A. Gordenin, E.N. Bergstrom, S.M.A. Islam, N. Lopez-Bigas, L.J. Klimczak, J.R. McPherson, S. Morganella, R. Sabarinathan, D. A. Wheeler, V. Mustonen, P.M.S.W. Group, G. Getz, S.G. Rozen, M.R. Stratton, P. Consortium, The repertoire of mutational signatures in human cancer, Nature 578 (2020) 94–101.
[20] L.B. Alexandrov, S. Nik-Zainal, D.C. Wedge, S.A. Aparicio, S. Behjati, A.V. Biankin, G.R. Bignell, N. Bolli, A. Borg, A.L. Borresen-Dale, S. Boyault, B. Burkhardt, A. P. Butler, C. Caldas, H.R. Davies, C. Desmedt, R. Eils, J.E. Eyfjord, J.A. Foekens, M. Greaves, F. Hosoda, B. Hutter, T. Ilicic, S. Imbeaud, M. Imielinski, N. Jager, D. T. Jones, D. Jones, S. Knappskog, M. Kool, S.R. Lakhani, C. Lopez-Otin, S. Martin, N.C. Munshi, H. Nakamura, P.A. Northcott, M. Pajic, E. Papaemmanuil, A. Paradiso, J.V. Pearson, X.S. Puente, K. Raine, M. Ramakrishna, A.L. Richardson, J. Richter, P. Rosenstiel, M. Schlesner, T.N. Schumacher, P.N. Span, J.W. Teague, Y. Totoki, A.N. Tutt, R. Valdes-Mas, M.M. van Buuren, L. van 't Veer, A. Vincent-Salomon, N. Waddell, L.R. Yates, I. Australian Pancreatic Cancer Genome, I.B. C. Consortium, I.M.-S. Consortium, I. PedBrain, J. Zucman-Rossi, P.A. Futreal, U. McDermott, P. Lichter, M. Meyerson, S.M. Grimmond, R. Siebert, E. Campo, T. Shibata, S.M. Pfister, P.J. Campbell, M.R. Stratton, Signatures of mutational processes in human cancer, Nature 500 (2013) 415–421.
[21] K. Sendowski, M.F. Rajewsky, DNA sequence dependence of guanine-O6 alkylation by the N-nitroso carcinogens N-methyl- and N-ethyl-N-nitrosourea, Mutat. Res 250 (1991) 153–160.
[22] M.E. Dolan, M. Oplinger, A.E. Pegg, Sequence specificity of guanine alkylation and repair, Carcinogenesis 9 (1988) 2139–2143.
[23] L. Haracska, S. Prakash, L. Prakash, Yeast DNA polymerase zeta is an efficient extender of primer ends opposite from 7,8-dihydro-8-Oxoguanine and O6-methylguanine, Mol. Cell Biol. 23 (2003) 1453–1459.
[24] L. Haracska, S. Prakash, L. Prakash, Replication past O(6)-methylguanine by yeast and human DNA polymerase eta, Mol. Cell Biol. 20 (2000) 8001–8007.
[25] L. Haracska, L. Prakash, S. Prakash, Role of human DNA polymerase kappa as an extender in translesion synthesis, Proc. Natl. Acad. Sci. USA 99 (2002) 16000–16005.
[26] H. Du, P. Wang, L. Li, Y. Wang, Repair and translesion synthesis of O(6)-alkylguanine DNA lesions in human cells, J. Biol. Chem. 294 (2019) 11144–11153.
[27] M.H. Raz, H.R. Dexter, C.L. Millington, B. van Loon, D.M. Williams, S.J. Sturla, Bypass of Mutagenic O(6)-Carboxymethylguanine DNA Adducts by Human Y- and B-Family Polymerases, Chem. Res Toxicol. 29 (2016) 1493–1503.
[28] M.H. Raz, S.J. Sturla, H.L. Gahlon, Hydrogen-Bonding Interactions at the DNA Terminus Promote Extension from Methylguanine Lesions by Human Extender DNA Polymerase zeta, Biochemistry 57 (2018) 5978–5988.
[29] W. Lin, X. Wu, Z. Wang, A full-length cDNA of hREV3 is predicted to encode DNA polymerase zeta for damage-induced mutagenesis in humans, Mutat. Res 433 (1999) 89–98.
[30] Y.S. Lee, M.T. Gregory, W. Yang, Human Pol zeta purified with accessory subunits is active in translesion DNA synthesis and complements Pol eta in cisplatin bypass, Proc. Natl. Acad. Sci. USA 111 (2014) 2954–2959.
[31] C.M.N. Aloisi, E.S. Sandell, S.J. Sturla, A Chemical Link between Meat Consumption and Colorectal Cancer Development? Chem. Res Toxicol. 34 (2021) 12–23.
[32] R. Smits, N. Hofland, W. Edelmann, M. Geugien, S. Jagmohan-Changur, C. Albuquerque, C. Breukel, R. Kucherlapati, M.F. Kielman, R. Fodde, Somatic Apc mutations are selected upon their capacity to inactivate the beta-catenin downregulating activity, Genes Chromosomes Cancer 29 (2000) 229–239.
[33] P.P. Van Sloun, I. Varlet, E. Sonneveld, J.J. Boei, R.J. Romeijn, J.C. Eeken, N. De Wind, Involvement of mouse Rev3 in tolerance of endogenous and exogenous DNA damage, Mol. Cell Biol. 22 (2002) 2159–2169.
[34] A.M. Dirac, R. Bernards, Reversal of senescence in mouse fibroblasts through lentiviral suppression of p53, J. Biol. Chem. 278 (2003) 11731–11734.
[35] H. Li, R. Durbin, Fast and accurate long-read alignment with Burrows-Wheeler transform, Bioinformatics 26 (2010) 589–595.
[36] A. Tarasov, A.J. Vilella, E. Cuppen, I.J. Nijman, P. Prins, Sambamba: fast processing of NGS alignment formats, Bioinformatics 31 (2015) 2032–2034.
[37] M.A. DePristo, E. Banks, R. Poplin, K.V. Garimella, J.R. Maguire, C. Hartl, A. A. Philippakis, G. del Angel, M.A. Rivas, M. Hanna, A. McKenna, T.J. Fennell, A. M. Kernytsky, A.Y. Sivachenko, K. Cibulskis, S.B. Gabriel, D. Altshuler, M.J. Daly, A framework for variation discovery and genotyping using next-generation DNA sequencing data, Nat. Genet 43 (2011) 491–498.
[38] M. Jager, F. Blokzijl, V. Sasselli, S. Boymans, R. Janssen, N. Besselink, H. Clevers, R. van Boxtel, E. Cuppen, Measuring mutation accumulation in single human adult stem cells by whole-genome sequencing of organoid cultures, Nat. Protoc. 13 (2018) 59–78.
[39] F. Manders, A.M. Brandsma, J. de Kanter, M. Verheul, R. Oka, M.J. van Roosmalen, B. van der Roest, A. van Hoeck, E. Cuppen, R. van Boxtel, , MutationalPatterns: the one stop shop for the analysis of mutational processes, BMC Genom. 23 (2022) 134.
[40] A.R. Lehmann, A. Niimi, T. Ogi, S. Brown, S. Sabbioneda, J.F. Wing, P. L. Kannouche, C.M. Green, Translesion synthesis: Y-family polymerases and the polymerase switch, DNA Repair (Amst.) 6 (2007) 891–899.
[41] O.J. Sansom, N.J. Toft, D.J. Winton, A.R. Clarke, Msh-2 suppresses in vivo mutation in a gene dose and lesion dependent manner, Oncogene 20 (2001) 3580–3584.
[42] O.V. Kochenova, D.L. Daee, T.M. Mertz, P.V. Shcherbakova, DNA polymerase zeta-dependent lesion bypass in Saccharomyces cerevisiae is accompanied by error-prone copying of long stretches of adjacent DNA, PLoS Genet 11 (2015) e1005110.
[43] K. Lehner, S. Jinks-Robertson, The mismatch repair system promotes DNA polymerase zeta-dependent translesion synthesis in yeast, Proc. Natl. Acad. Sci. USA 106 (2009) 5749–5754.
[44] W. Xiao, L. Rathgeber, T. Fontanie, S. Bawa, DNA mismatch repair mutants do not increase N-methyl-N′-nitro-N-nitrosoguanidine tolerance in O6-methylguanine DNA methyltransferase-deficient yeast cells, Carcinogenesis 16 (1995) 1933–1939.
[45] H. Saribasak, R.W. Maul, Z. Cao, W.W. Yang, D. Schenten, S. Kracker, P. J. Gearhart, DNA polymerase zeta generates tandem mutations in immunoglobulin variable regions, J. Exp. Med 209 (2012) 1075–1081.
[46] M. Touat, Y.Y. Li, A.N. Boynton, L.F. Spurr, J.B. Iorgulescu, C.L. Bohrson, I. Cortes-Ciriano, C. Birzu, J.E. Geduldig, K. Pelton, M.J. Lim-Fat, S. Pal, R. Ferrer-Luna, S. H. Ramkissoon, F. Dubois, C. Bellamy, N. Currimjee, J. Bonardi, K. Qian, P. Ho, S. Malinowski, L. Taquet, R.E. Jones, A. Shetty, K.H. Chow, R. Sharaf, D. Pavlick, L. A. Albacker, N. Younan, C. Baldini, M. Verreault, M. Giry, E. Guillerm, S. Ammari, F. Beuvon, K. Mokhtari, A. Alentorn, C. Dehais, C. Houillier, F. Laigle-Donadey, D. Psimaras, E.Q. Lee, L. Nayak, J.R. McFaline-Figueroa, A. Carpentier, P. Cornu, L. Capelle, B. Mathon, J.S. Barnholtz-Sloan, A. Chakravarti, W.L. Bi, E.A. Chiocca, K.P. Fehnel, S. Alexandrescu, S.N. Chi, D. Haas-Kogan, T.T. Batchelor, G. M. Frampton, B.M. Alexander, R.Y. Huang, A.H. Ligon, F. Coulet, J.Y. Delattre, K. Hoang-Xuan, D.M. Meredith, S. Santagata, A. Duval, M. Sanson, A.D. Cherniack, P.Y. Wen, D.A. Reardon, A. Marabelle, P.J. Park, A. Idbaih, R. Beroukhim, P. Bandopadhayay, F. Bielle, K.L. Ligon, Mechanisms and therapeutic implications of hypermutation in gliomas, Nature 580 (2020) 517–523.
[47] M.T. Latancia, N.C. Moreno, G.S. Leandro, V.C. Ribeiro, I. de Souza, W.K.M. Vieira, A.U. Bastos, N.C. Hoch, C.R.R. Rocha, C.F.M. Menck, DNA polymerase eta protects

human cells against DNA damage induced by the tumor chemotherapeutic temozolomide, Mutat. Res Genet Toxicol. Environ. Mutagen 878 (2022) 503498.
[48] O. Pich, F. Muinos, M.P. Lolkema, N. Steeghs, A. Gonzalez-Perez, N. Lopez-Bigas, The mutational footprints of cancer therapies, Nat. Genet 51 (2019) 1732–1740.
[49] D.J. Brierley, S.A. Martin, Oxidative stress and the DNA mismatch repair pathway, Antioxid. Redox Signal 18 (2013) 2420–2428.
[50] B. Pilzecker, H. Jacobs, Mutating for Good: DNA Damage Responses During Somatic Hypermutation, Front Immunol. 10 (2019) 438.
[51] A. Tsaalbi-Shtylik, C. Ferras, B. Pauw, G. Hendriks, P. Temviriyanukul, L. Carlee, F. Calleja, S. van Hees, J. Akagi, S. Iwai, F. Hanaoka, J.G. Jansen, N. de Wind, Excision of translesion synthesis errors orchestrates responses to helix-distorting DNA lesions, J. Cell Biol. 209 (2015) 33–46.